



Faculty of Mechanical Engineering



**STABILITY ANALYSIS OF CONE-CYLINDER SHELL
STRUCTURES**

Mohd Shahrom bin Ismail

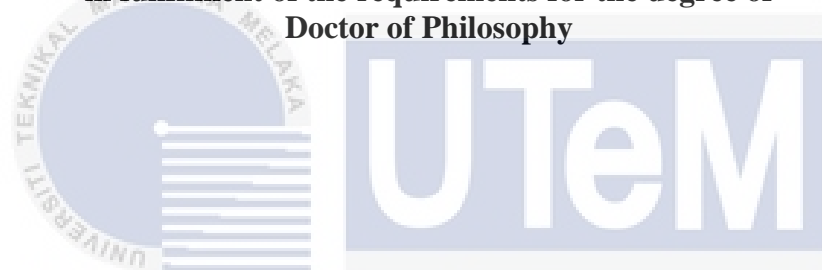
Doctor of Philosophy

2021

STABILITY ANALYSIS OF CONE-CYLINDER SHELL STRUCTURES

MOHD SHAHROM ISMAIL

A thesis submitted
in fulfillment of the requirements for the degree of
Doctor of Philosophy



اونيورسيتي تكنولوجيک ماليسيا ملاک
Faculty of Mechanical Engineering

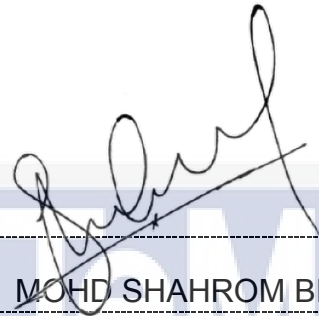
UNIVERSITI TEKNIKAL MALAYSIA MELAKA

UNIVERSITI TEKNIKAL MALAYSIA MELAKA

2021

DECLARATION

I declare that this thesis entitled “Stability Analysis of Cone-Cylinder Shell Structures” is the result of my own research except as cited in the references. The thesis has not been accepted for any degree and is not concurrently submitted in candidature of any other degree.

Signature : 
Name : MOHD SHAHROM BIN ISMAIL
Date : 20 OGOS 2021

اونيورسيتي تيكنيكل مليسيا ملاك

UNIVERSITI TEKNIKAL MALAYSIA MELAKA

APPROVAL

I hereby declare that I have checked this thesis and in my opinion, this thesis is adequate in terms of scope and quality for the award of the degree of Doctor of Philosophy.

Signature :

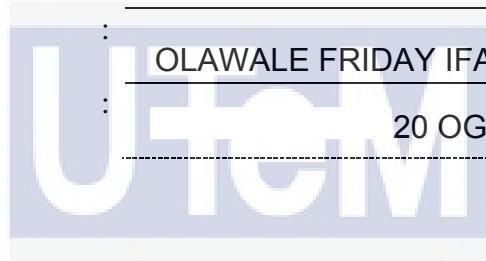
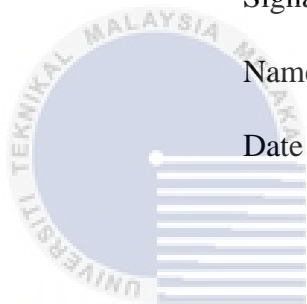


Name :

OLAWALE FRIDAY IFAYEFUNMI

Date :

20 OGOS 2021



اونيورسيتي تيكنيكل مليسيا ملاك

UNIVERSITI TEKNIKAL MALAYSIA MELAKA

DEDICATION

Untuk para pencinta ilmu, moga pahala yang diperolehi menerusi laporan ini berterusan.



ABSTRACT

This thesis presents an evaluation of the structural performance that is relevant to the application in major industries globally (for example, oil platform, submersible structures, some compartment in aircraft/aerospace structures, shipbuilding, bridges, and others.), against failure/collapse. This structure is susceptible to buckling failures caused by excessive mechanical load action. During the design process or the buckling failure evaluation of this particular structure, initial geometric and loading imperfections are of important parameters for the analyses. Therefore, the engineers/designers are expected to well understand the physical behaviours of shell buckling to prevent unexpected serious failure in structures. In particular, it is widely reported that no efficient guidelines for modelling imperfections in particular structures are available. The consequence of inadequate design knowledge may result in (a) loss of life, (b) loss of properties and belongings, (c) costly financial implication, (d) loss of time, and (e) pollution. Therefore, knowledge obtained from the relevant works is open for updates and highly sought. In this study, the structural performance under bifurcation and collapse load, the role of ring stiffener reinforcement (such as, internal and externally stiffened), the influence of structural plasticity, and the worst-case of the imperfection for (i) cone-cylinder and (ii) cylinder-cone-cylinder shells transition have been comprehensively studied, presented and discussed. The cone-cylinder shell has also been tested experimentally to (i) axial compression and (ii) combination of axial compression and thermal. To support the experimental results, numerical simulations of cone-cylinder and cylinder-cone-cylinder transition shells are conducted by use of a finite element (FE) method based software of ABAQUS. Initial geometric imperfection techniques such as (i) eigenmode imperfection, (ii) SPLA (Single Perturbation Load approach), MPLA (Multiple Perturbation Load approach), and axisymmetric outward bulged were also adopted to further evaluate the shells worst case of imperfection under various mechanical loads. It worth noting that in this study, the establishment of the (i) design guideline and (ii) lower bound knockdown factor for a combination of shell structure assembly subjected to (i) external pressure and (ii) axial compression are presented. In particular, with a consideration of practical interest, cone-cylinder transition shell under combined load action (such as, (i) axial compression and thermal and (ii) axial compression and external pressure) were further examined through experimentation and numerical analysis. Subsequently, there is a good agreement between experimental and numerically predicted collapse load with discrepancy calculated to be within 10%. Several recommendations in the area of the structural design against collapse/failure were underline and proposed accordingly throughout the analysis.

ANALISA KESTABILAN STRUKTUR KELOMPANG KON-SILINDER

ABSTRAK

Tesis ini membentangkan penilaian ke atas prestasi struktur yang berkaitan dengan pengaplikasiannya dalam industri utama di dunia (contohnya, platform minyak, struktur tenggelam, beberapa ruang didalam struktur pesawat udara/aeroangkasa, pembinaan kapal, jambatan, dan pelbagai lagi), dalam menghadapi proses lengkohan. Umum mengetahui, struktur ini mudah terjejas akibat kegagalan bebanan mekanikal yang berlebihan. Semasa proses mereka bentuk struktur, unsur ketaksempurnaan geometri awalan adalah penting untuk dianalisis dan difahami. Oleh itu, jurutera/pereka adalah diharap untuk lebih memahami fizikal lengkohan kelompang bagi mengelakkan kegagalan yang serius pada struktur. Sehingga kini, dilaporkan bahawa tiada garis panduan yang efisien untuk mengadaptasi kaedah permodelan sifat ketaksempurnaan kelompang. Kesan daripada isu lengkohan ini boleh mengakibatkan (a) kehilangan nyawa, (b) kehilangan harta benda, (c) implikasi kewangan, (d) kehilangan masa, dan (e) pencemaran. Oleh itu, pengetahuan yang diperoleh daripada kerja-kerja yang berkaitan ini sentiasa terbuka untuk dikemas kini. Prestasi struktur di bawah mod bifurkasi dan beban runtuh, peranan pengukuh/tetulang secara lilitan (dalaman dan luaran), pengaruh plastik struktur, dan kes terburuk bagi (i) kon-silinder dan (ii) silinder-kon-silinder telah dipelajari, dibentangkan dan dibincangkan. Kelompang kon-silinder juga diuji secara eksperimental dengan (i) beban mampatan paksi menegak dan (ii) gabungan beban mampatan paksi menegak dan haba. Untuk menyokong hasil keputusan ujikaji, simulasi model berkomputer yang melibatkan kon-silinder dan silinder-kon-silinder dilaksanakan dengan menggunakan perisian berasaskan kaedah unsur terhingga ABAQUS. Teknik-teknik ketaksempurnaan geometri awalan seperti (i) ketaksempurnaan eigenmode, (ii) SPLA (pendekatan daya usikan tunggal), (iii) MPLA (pendekatan daya usikan pelbagai), dan (iv) bebanan paksi simetri luaran juga digunakan untuk penilaian yang lebih lanjut bagi mengambil kira kes-kes terburuk di bawah pelbagai bebanan mekanikal. Adalah diingatkan bahawa dalam kajian ini, penetapan (i) garis panduan reka bentuk dan (ii) batasan bawah untuk kes gabungan kelompang pelbagai yang dikenakan daya (i) tekanan luaran dan (ii) beban mampatan paksi menegak dibentangkan. Dengan mempertimbangkan kepentingan secara praktikal, kon-silinder nipis ini juga diuji di bawah beban gabungan yang terdiri daripada (i) beban mampatan paksi menegak dan terma (suhu tinggi) dan (ii) beban mampatan paksi menegak dan tekanan luaran diperiksa selanjutnya melalui kaedah eksperimen dan analisis berangka. Perbezaan nilai beban runtuh melalui dapatan kaedah eksperimen dan analisis berangka adalah dalam lingkungan 10%. Sepanjang analisa, beberapa cadangan khususnya dalam bidang reka bentuk struktur terhadap isu lengkohan telah digariskan dan dicadangkan dengan sewajarnya.

ACKNOWLEDGEMENT

In the Name of Allah, the Most Gracious, the Most Merciful

First and foremost, all praise goes to Allah the Almighty, my Creator, my Sustainer, for everything I received since the beginning of my life. I would like to extend my appreciation to Bahagian Kompetensi dan Peningkatan Kerjaya, Jabatan Pendidikan Politeknik dan Kolej Komuniti (BKPK, JPPKK) and Universiti Teknikal Malaysia Melaka (UTeM) for providing the research platform. I would like to express my gratitude to the Ministry of Higher Education (MOHE) of Malaysia for the support and financial assistance.

My utmost appreciation goes to Dr. Olawale Friday Ifayefunmi, Fakulti Teknologi Kejuruteraan Mekanikal Dan Pembuatan, who has been abundantly helpful with invaluable assistance, support and guidance throughout this journey. Also, to Dr. Siti Hajar Binti Sheikh Md Fadzullah, from Fakulti Kejuruteraan Mekanikal for her constant support.

My special thanks to Mr. Amirul Husaini bin Mazli and Mr. Muhammad Zafri Ariffin bin Othman for all the help and technical support that I received from them.

Last but not least, from the bottom of my heart gratitude is fully addressed to my beloved wife, Siti Syazlina Alyssa binti Alias, for her encouragements and who has been the pillar of strength in all my life. My eternal love also dedicated to all my children, Adam, Ali, Arif, and Amir for their patience and understanding. Not to forget, my sincere appreciation also goes to my maid for her relentless help and care for the family during my absence. I would also like to thank my beloved parents for their endless support, love and prayers. Finally, thank you to all the individual(s) who had provided me with the assistance, support and inspiration to embark on my study. I will forever be grateful to them for all that they have given me.

TABLE OF CONTENTS

	PAGE
DECLARATION	
DEDICATION	
ABSTRACT	i
ABSTRAK	ii
ACKNOWLEDGEMENTS	iii
TABLE OF CONTENTS	iv
LIST OF TABLES	vii
LIST OF FIGURES	ix
LIST OF SYMBOLS AND ABBREVIATIONS	xx
LIST OF APPENDICES	xxiii
LIST OF PUBLICATIONS	xxiv
CHAPTER	
1. INTRODUCTION	1
1.1 Background	1
1.1.1 Overview of the development of shell buckling theory	3
1.2 Problem Statement	5
1.3 Research Objective	6
1.4 Scope of Research	6
1.5 Contribution of Research	7
1.6 Thesis Outline	8
2. LITERATURE REVIEW	10
2.1 Overview	10
2.2 Shell buckling: background of failure structures	11
2.3 Cone-cylinder transition under internal pressure	16
2.3.1 Background and application	16
2.3.2 Past finding	17
2.3.3 Summary of finding	21
2.4 Cone-cylinder under external pressure	24
2.4.1 Background and application	24
2.4.2 Past finding	25
2.4.3 Summary of finding	27
2.5 Cone-cylinder transition under axial compression	28
2.5.1 Background and application	28
2.5.2 Past finding	30
2.5.3 Summary of finding	31
2.6 Shells imperfection and its design implication	33
2.7 Some commentary on current design practice: initial imperfection	38
2.8 Review of available imperfection approach	44
2.8.1 Measurement of a shell that deviated from perfect geometry	44
2.8.2 Eigenmode imperfection	46
2.8.3 Single and multiple perturbation load approaches	49
2.8.4 Imperfect length, boundary condition, and load	54

eccentricities	
2.8.5 Residual stress and its imperfection	58
2.9 Shell subjected to thermal loading	60
2.10 Summary	62
3. METHODOLOGY	64
3.1 Introduction	64
3.2 Research design	66
3.3 List of testing equipment and facilities	72
3.4 Numerical simulations	72
3.4.1 Finite element method (FEM)	73
3.5 Buckling of imperfect cone-cylinder transition subjected to external pressure	76
3.5.1 Preliminary studies	77
3.5.2 Imperfect cone-cylinder transition – Eigenmode shape and SPLA imperfection	82
3.5.3 Proposed guideline for cone-cylinder shell transition	86
3.6 Buckling analysis of stiffened cone-cylinder intersection subjected to external pressure	87
3.6.1 Geometry and material	88
3.6.2 Finite element modelling and boundary condition	89
3.7 Buckling of imperfect cylinder-cone-cylinder transition under axial compression	90
3.7.1 Numerical modelling	91
3.7.2 Imperfect cylinder-cone-cylinder transition – Eigenmode shape, Axisymmetric inward/outward bulged and SPLA imperfection	94
3.8 Cone-cylinder shell - experimentation	98
3.8.1 The fabrication process, pre-test and material properties	98
3.8.2 Setting-up of the collapse test	105
3.9 Cone-cylinder shell - numerical modelling	109
3.9.1 Buckling of the perfect cone-cylinder shell under axial compression	109
3.9.2 Buckling of the perfect cone-cylinder shell under combined loading – axial compression and thermal	111
3.9.3 Buckling of the imperfect cone-cylinder shell under combined loading – axial compression and thermal	114
3.9.4 Buckling of the perfect cone-cylinder shell under combined loading – axial compression and external pressure	115
3.10 Limitation of the proposed methodology	116
3.11 Summary	117
4. RESULTS AND DISCUSSION	118
4.1 Introduction	118
4.2 Buckling of imperfect cone-cylinder transition subjected to external pressure	118
4.2.1 Preliminary studies	119
4.2.2 Imperfect cone-cylinder transition – Eigenmode shape and SPLA imperfection	123

4.2.3	Comparison between Eigenmode shape and SPLA imperfection	130
4.2.4	Proposed guideline for cone-cylinder shell transition	134
4.3	Buckling analysis of stiffened cone-cylinder intersection subjected to external pressure	138
4.3.1	Buckling of stiffened cone-cylinder intersection under external pressure: numerical results	138
4.4	Buckling of imperfect cylinder-cone-cylinder transition under axial compression	142
4.4.1	Numerical modelling with validation results	142
4.4.2	The failure mechanism of cylinder-cone-cylinder	143
4.4.3	Imperfect cylinder-cone-cylinder transition – Eigenmode shape, Axisymmetric inward/outward bulged and SPLA imperfection	147
4.4.4	Comparison between Eigenmode shape, Axisymmetric inward bulged and SPLA imperfection	155
4.4.5	The lower bound knockdown factor for design purpose	156
4.5	Cone-cylinder shell - experimentation	159
4.5.1	Collapse test and results – axial compression	159
4.5.2	Collapse test and results – combined loading of axial compression and thermal	162
4.6	Cone-cylinder shell - numerical results	165
4.6.1	Comparison of experimental and numerical results for cone-cylinder subjected to axial compression	165
4.6.2	Comparison of experimental and numerical results for cone-cylinder subjected to combined loading of axial compression and thermal	162
4.6.3	Plastic analysis of cone-cylinder shell subjected to combined axial compression and thermal loading	172
4.6.4	Buckling of the imperfect cone-cylinder shell under combined loading – axial compression and thermal	174
4.6.5	Numerical predictions for cone-cylinder shell buckling caused by axial compression or by external pressure	177
4.6.6	Numerical predictions for cone-cylinder shell subjected to combined axial compression and external pressure	180
4.7	Summary	193
5.	CONCLUSION AND RECOMMENDATION FOR FUTURE RESEARCH	194
5.1	Conclusion	194
5.2	Recommendations for future research	198
	REFERENCES	201
	APPENDICES	223

LIST OF TABLES

TABLE	TITLE	PAGE
2.1	Shell geometrical tolerance from selected design codes	42
2.2	Stiffened shells geometrical tolerance from selected design codes	43
3.1	List of equipment/facilities and their availability	72
3.2	Geometrical properties of analyzed models in referring to (Galletly et al., 1974)	79
3.3	Four types of boundary conditions (BC) applied at the equatorial (bottom) plane of the cone-cylinder intersection, for example, type '1' means fully clamped support. Note $c \equiv$ variable is set to zero, $f \equiv$ variable is set to free	70
3.4	The effect of boundary conditions on cone-cylinder intersections collapse pressure and magnitude of bifurcation N.B: (*) Axisymmetrical buckles	79
3.5	Convergence study of externally pressurized cone-cylinder shell transition for model no. 1	81
3.6	Geometrical properties of analyzed models in referring to (Galletly et al., 1974) with additional stiffeners used in the study	89
3.7	Geometrical properties of analysed models in referring to (ECCS, 1998)	91
3.8	Material properties used in the analysis is referring to (ECCS, 1998)	92

3.9	Results of the mesh sensitivity for the benchmarked models	94
3.10	Set of material data obtained from uniaxial tensile tests on a mild steel plate (E = Young's modulus, σ_{yield} = yield stress, and UTS = Ultimate Tensile Strength)	100
3.11	Measured data of the wall thickness for all tested cone-cylinder specimens	102
3.12	Average measured geometry of cone-cylinder shells (mid-surface values where appropriate)	102
3.13	Measured data of the wall thickness for all tested cone-cylinder specimens	104
3.14	Average measured geometry of cone-cylinder shells (mid-surface values where appropriate)	104
3.15	Numerical result of mesh sensitivity exemplify by model CC2a-AC	111
3.16	Numerical result of mesh sensitivity for model CC5	113
4.1	Comparison of experimental and numerical results for the externally pressurized cone-cylinder transition. The number in parenthesis is $P_{\text{extpl}}/P_{\text{num}}$	120
4.2	Comparison of experimental and numerical results for the axially compressed cylinder-cone-cylinder transition. The number in parenthesis is $F_{\text{extpl}}/F_{\text{coll}}$	143
4.3	Comparison of experimental and numerical results for cone-cylinder shells subjected to axial compression	160
4.4	Comparison of experimental and numerical results for cone-cylinder shells under combined axial compression with temperature (A = Gillie model and B = ECCS)	163

LIST OF FIGURES

FIGURE	TITLE	PAGE
1.1	Structure of (a) FGD vessel and (b) geometry of cone-cylinder transition subjected to axial compression load (Schmidt, 2018)	2
2.1	(a) The water tower (such as,, elevated conical tank) located at Fredericton, New Brunswick, Canada and (b) its collapsed (Dawe et al., 1993)	12
2.2	(a) The failed accident of 16 years old silo (Piskoty et al., 2005) and (b) the buckled of a vertical column of an empty silo that located at Poland (Iwicki et al., 2011)	13
2.3	An example of Yoshimura buckling pattern (Yoshimura, 1955)	15
2.4	The buckling pattern of (a) thick cylinder (Ifayefunmi, 2016) and (b) thin cylinder with “chess-board” pattern (Lancaster et al., 2000)	15
2.5	(a) The buckled of cone-cylinder intersection under internal pressure and (b) the structure at post-buckle state (Teng and Zhao, 2000)	17
2.6	Specimen ZKZ-XV10: (a) after testing, (b) LBA buckling mode and (c) GNA buckling mode (Schmidt, 2018)	32
2.7	The stability curve of NASA SP-8007 together with available test data	40

	(Friedrich and Schröder, 2016)	
2.8	The example of shell stability curve of based on ECCS design guideline (ECCS, 2008)	42
2.9	Tolerance measurement for imperfections (Rotter, 2017)	43
2.10	Sketch of cylinder shell that under imperfection measurement (Elghazouli et al., 1998)	45
2.11	Typical result of the shell's thickness measurement (Elghazouli et al., 1998)	46
2.12	Eigenmode imperfection of cone subjected to (a) axial compression, (b) external pressure, and (c) combine loading of both (Ifayefunmi and Błachut, 2013)	48
2.13	Reduction of load-carrying capacity in the function of amplitude-to- thickness ratio for cone subjected to external pressure (Ifayefunmi and Błachut, 2013)	48
2.14	The initial imperfection approaches: (a) the SPLA (Ismail et al., 2015), (b) MPLA (Arbelo et al., 2014)	50
2.15	The knockdown factors derived from (a) the SPLA (Ismail et al., 2015) and (b) MPLA (Arbelo et al., 2014)	51
2.16	An overview of perturbation approaches together with their respective reaction loads (a) SPLA, (ii) SPDA, and (iii) SBPA (Wagner et al., 2017a)	53
2.17	Illustration of an axially compressed cylinder by a rigid disk together with	55

	boundary condition (Błachut, 2010)	
2.18	Typical imperfection sensitivity of uneven length of a steel cylinder with various amplitude-thickness ratio (Ifayefunmi and Błachut, 2018)	56
3.1	Research workflow of cone-cylinder shell subjected to external pressure	68
3.2	Research workflow of ring-stiffened cone-cylinder subjected to external pressure	79
3.3	Research workflow of cylinder-cone-cylinder shell subjected to axial compression	70
3.4	Research workflow of experimental and numerical analysis of cone-cylinder shell subjected to various load action	71
3.5	Geometry of cone-cylinder transition subjected to external pressure	78
3.6	Illustration of imperfection shape exemplified for model no. 2 (a) Eigenmode, (b) SPLA-cylinder mid-section, (c) SPLA-cone mid-section and (d) SPLA-cone & cylinder mid-section	85
3.7	Buckling mode shapes, $n = 1, \dots, 5$, for cone-cylinder transition subjected to external pressure (model no. 1)	85
3.8	(a) Geometry of the analyzed stiffened cone-cylinder intersection subjected to (b) external pressure	89
3.9	(a) – (c) the numerical model of the cone-cylinder assembly strengthening with stiffener have cone angle, $\beta = 45^\circ$, $\beta = 60^\circ$ and $\beta = 75^\circ$ (figure not to scaled)	90

3.10	Geometry of cylinder-cone-cylinder transition subjected to axial compression	92
3.11	Illustration of imperfection shape for (a) Eigenmode, (b) SPLA-cone midsection, (c) SPLA bottom cylinder midsection, (d) SPLA-top cylinder midsection and (e) Axisymmetric outward bulged	96
3.12	Buckling mode shapes, $n = 1, \dots, 7$, for cylinder-cone-cylinder transition subjected to axial compression	97
3.13	(a) Geometry and boundary condition of cone-cylinder shell subjected to axial compression and (b) combined between axial compression and external pressure. N.B: 'F' = axial compression and 'P' = external pressure	99
3.14	A plot of stress-strain tensile test exemplified by H1 specimen	101
3.15	(a) Geometry of cone-cylinder shell subjected to thermal load and axial compression. (b) Photograph of as-fabricated cone-cylinder	105
3.16	Test set-up for cone-cylinder specimen under axial compression	108
3.17	Plot of load versus compression extension for cone-cylinder specimen CC1 subjected to axial compression	108
3.18	Test set-up for cone-cylinder specimen under combined axial compression and temperature using the temperature chamber	109
3.19	Variation of Elastic modulus with temperature	112
3.20	Variation of yield stress with temperature	112

4.1	Comparison of numerically obtained buckling pressure with experimental results for cone-cylinder model no. 1, 2, and 3 in (Galletly et al., 1974)	120
4.2	Plot of load versus deflection of externally pressurized cone-cylinder intersections for perfect model no. 1, 2 and 3	122
4.3	Numerically calculated of critical load, P_{crit} for cone-cylinder shell against cone and cylinder shells with a range of dimensionless ratios of $50 < r_{cyl}/t < 450$	122
4.4	Effect of imperfection amplitude and Eigenmode on the buckling strength of the cone-cylinder transition with cone angle, $\beta = 45^\circ$ (model no. 1)	125
4.5	Load-deflection curves for point (A) in Figure 4.4 and perfect cone-cylinder shell with cone angle, $\beta = 45^\circ$ (model no. 1)	125
4.6	Effect of imperfection amplitude and Eigenmode on the buckling strength of the cone-cylinder transition with cone angle, $\beta = 60^\circ$ (model no. 2)	126
4.7	Load-deflection curves for point (B) in Figure 4.6 and perfect cone-cylinder shell with cone angle, $\beta = 60^\circ$ (model no. 2)	126
4.8	Effect of imperfection amplitude and Eigenmode on the buckling strength of the cone-cylinder transition with cone angle, $\beta = 75^\circ$ (model no. 3)	127
4.9	Load-deflection curves for point (C) in Figure 4.8 and perfect cone-cylinder shell with cone angle, $\beta = 75^\circ$ (model no. 3)	127
4.10	Effect of imperfection amplitude and SPLA on the buckling strength of the cone-cylinder transition with cone angle, $\beta = 45^\circ$ (model no. 1)	129

4.11	Effect of imperfection amplitude and SPLA on the buckling strength of the cone-cylinder transition with cone angle, $\beta = 60^\circ$ (model no. 2)	129
4.12	Effect of imperfection amplitude and SPLA on the buckling strength of the cone-cylinder transition with cone angle, $\beta = 75^\circ$ (model no. 3)	130
4.13	Reduction of buckling strength as a function of imperfection amplitude, w_0/t . Comparison of worst Eigenmode and worst SPLA for a cone-cylinder transition with $\beta = 45^\circ$ (model no. 1)	132
4.14	Reduction of buckling strength as a function of imperfection amplitude, w_0/t . Comparison of worst Eigenmode and worst SPLA for a cone-cylinder transition with $\beta = 60^\circ$ (model no. 2)	132
4.15	Reduction of buckling strength as a function of imperfection amplitude, w_0/t . Comparison of worst Eigenmode and worst SPLA for a cone-cylinder transition with $\beta = 75^\circ$ (model no. 3)	133
4.16	Effect of cone angle on the buckling behaviour of imperfect cone-cylinder transition such as, cone angle, β , ranges from 45° to 75°	133
4.17	The proposed design guideline curve with empirical formulae for the case of (a) perfect (GMNA) and (b) imperfect (GMNIA) cone-cylinder shell transitions subjected to external pressure	136
4.18	Comparison of the proposed equation with the numerical result for the case of (a) perfect (GMNA) and (b) imperfect (GMNIA) cone-cylinder shell transitions subjected to external pressure	137

4.19	The effect of (a) internally ring-stiffened ($N_r = 1$) and (b) externally ring-stiffened cone-cylinder intersections subjected to external pressure with a different set of case	140
4.20	The effect of buckling load against cone angle at (a) $\beta = 45^\circ$, (b) $\beta = 60^\circ$ and (c) $\beta = 75^\circ$ for internally and externally ring-stiffened ($N_r = 1$) cone-cylinder intersections under external pressure	141
4.21	Plot of load versus deflection of axially compressed cylinder-cone-cylinder intersections for a perfect model	145
4.22	Plot of elastic and elastic-plastic load versus deflection of axially compressed cylinder-cone-cylinder intersections for perfect model ZKZ-XV50	145
4.23	Spread of plastic strain at yield and collapse for cylinder-cone-cylinder transitions under axial compression	146
4.24	Effect of imperfection amplitude and Eigenmode on the buckling strength of the cylinder-cone-cylinder transition	149
4.25	Reduction of buckling strength as a function of imperfection amplitude, w_0/t . Comparison of imperfection amplitude between the worst imperfection approaches: Eigenmode Analysis and Axisymmetric outward bulged curves	149
4.26	Load-deflection curves for point (A) and (B) in Figure 4.25 with perfect cylinder-cone-cylinder shell	150

4.27	Plot of perfect and imperfect load versus deflection curve of axially compressed cylinder-cone-cylinder intersections using elastic material modelling behaviour	150
4.28	Plot of perfect and imperfect load versus deflection curve of axially compressed cylinder-cone-cylinder intersections using elastic perfectly plastic material modelling behaviour	151
4.29	Effect of imperfection amplitude and SPLA on the buckling strength of the cylinder-cone-cylinder transition	153
4.30	(a) Full structure assembly with boundary condition and (b) location of applied lateral load along the cone slant length	153
4.31	Imperfection sensitivity of buckling load to the SPLA along the cone slant	154
4.32	Load-deflection curve for point (C) in Figure 4.31 for cylinder-cone-cylinder transition with SPLA imperfection having imperfection amplitude, $w_0/t = 4$	154
4.33	Reduction of buckling strength as a function of imperfection amplitude, w_0/t . Comparison of imperfection amplitude between the worst Eigenmode imperfections, axisymmetric outward bulged, MPLA and SPLA curves	156
4.34	Effect of imperfection amplitude and Eigenmode on the buckling strength of cylinder-cone-cylinder transition with different cone angles	158
4.35	Plot of worst imperfection (eigenmode) knockdown factor for cylinder-	158

	cone-cylinder transition having different cone radius-to-thickness ratio, r_{cone}/t	
4.36	Plot of load versus compression extension for cone-cylinder specimen CC2a-AC subjected to axial compression only	161
4.37	Photograph of selected cone-cylinders specimens after testing	161
4.38	Plot of load versus compression extension for the cone-cylinder specimen with different initial temperature subjected to axial compression	163
4.39	Effect of elevated temperature on the buckling load of axially compressed cone-cylinder shells	164
4.40	Photograph of all cone-cylinders specimens after testing	164
4.41	Comparison of numerically obtained buckling load with experimental results for cone-cylinder models	166
4.42	Combined stability plot for cone-cylinder with, $r_{\text{cyl}}/t = 72.19$, subjected to axial compression and thermal load	169
4.43	Plot of axial compressive force against compression extension for cone-cylinder shell subjected to axial compression only	169
4.44	Plot of axial compressive force against axial displacement for cone- cylinder shell subjected to combined axial compression and thermal load	170
4.45	Combined stability plot for cone-cylinder with different r_{cyl}/t , subjected to axial compression and thermal load	170
4.46	Combined stability plot for cone-cylinder with different cone angle, β ,	171

- subjected to axial compression and thermal load
- 4.47 Combined stability plot for cone-cylinder with different L_{cyl}/r_{cyl} , 171
 subjected to axial compression and thermal load
- 4.48 Dimensionless ratio of deformation-over-thickness of the cone-cylinder 173
 shell before reaching the collapse and post-collapse corresponding at 50%
 of collapse magnitude under a condition of temperature
 (T = ambient and T = 250°C)
- 4.49 Cone-cylinder shell structure distribution of (a) plastic strain and 174
 (b) stresses before reaching the collapse and post-collapse condition
 corresponding at 50% of collapse magnitude under a condition of
 temperature (T = ambient and T = 250°C)
- 4.50 Typical combined stability interaction curve of (a) perfect and 176
 (b) imperfection cone-cylinder shell subjected to axial compression
 and thermal loading
- 4.51 Plot of collapse load of cone-cylinder shell subjected to axial compression 179
 against (a) dimensionless-radius-to-thickness ratio and (b) cone angle.
 The plot of collapse/bifurcation load of cone-cylinder shell subjected to
 external pressure against (c) dimensionless-radius-to-thickness ratio and
 (d) cone angle
- 4.52 Typical combined stability plot for cone-cylinder transition of 181
 $r_{cyl}/r_{cone} = 1.75$, $r_{cyl}/t = 72.19$, and $\beta = 16.89^\circ$

- 4.53 Plot of load versus deflection of cone-cylinder shell subjected to 182
 (a) axially compressed, (b) externally pressurized and, (c) combined of
 both loads. The boundary condition of the shell under (d) combined
 loading
- 4.54 Dimensionless ratio of plastic deformation-over-thickness (such as, w/t) 184
 of a cone-cylinder shell at peak/collapse load prior to (i) axial compression,
 (ii) external pressure and, (iii) combination of both
- 4.55 Combined stability plot for cone-cylinder transition shell in the range 186
 of $50 < r_{cyl}/t < 400$ with constant $\beta = 10^\circ$
- 4.56 Domain of combined stability plot for different r_{cyl}/t values 187
- 4.57 Combined stability plot for cone-cylinder transition shell in the range 189
 of $10^\circ < \beta < 30^\circ$ with constant $r_{cyl}/t = 72.19$ and $r_{cyl}/r_{cone} = 1.75$
- 4.58 Domain of combined stability plot for different cone angle, β values 190
- 4.59 Plot of the area of plastic strains within the combined stability domain to 192
 the total area, against (a) dimensionless-radius-to-thickness ratio and
 (b) cone radius angle